Acta Cryst. (1975). B31, 2649

Electronic Structure of Chromium Hexacarbonyl at 78 K. I. Neutron Diffraction Study

BY ANNETTE JOST AND BERNARD REES

Laboratoire de Cristallochimie, Institut de Chimie, B.P. 296/R8, 67008 Strasbourg Cedex, France

AND WILLIAM B. YELON

Institut Max von Laue–Paul Langevin, B.P. 156 Centre de Tri, 38042 Grenoble Cedex, France

(*Received* 3 *March* 1975; *accepted* 23 *April* 1975)

The distribution of the nuclei of chromium hexacarbonyl $Cr(CO)_6$ in the crystalline state was refined from neutron diffraction data at 78 K. It was found that diffraction by the aluminum walls of the cryostat used for low-temperature measurements was superimposed on the diffraction peaks of the crystal, and a method was derived to correct for this effect. Extinction was rather severe, and the correction formulae recently derived by Becker & Coppens [*Acta Cryst.* (1974). A30, 129–153] were applied successfully in the least-squares refinements. The $Cr(CO)_6$ octahedron is significantly distorted in the crystal, but no significant differences were found between chemically equivalent bond lengths. The average values, directly derived by a least-squares procedure from the observed structure factors, and corrected for riding motion around chromium, are: Cr–C = 1·918 Å and C–O = 1·141 Å. These values show that the carbonyl groups are less strongly bonded to chromium than in the related complex benzene chromium tricarbonyl, which is consistent with the larger electronegativity of the carbonyl groups, compared to benzene.

Introduction

This work is the first part of an experimental study of the electron density in chromium hexacarbonyl $Cr(CO)_6$. It was undertaken to determine as precisely as possible the distribution of the nuclei in the crystal. The results of the X-ray study at the same temperature and a discussion of the electronic structure will be published later.

Our aim is the study of the metal–ligand bond in one of the simplest transition-metal complexes. Previous work on benzene chromium tricarbonyl (Rees & Coppens, 1973) had shown that it was not unreasonable to expect interesting results from combined X-ray and neutron diffraction measurements on compounds containing a transition metal of the first series.

To avoid as much as possible the smearing out of the electron density, and to minimize anharmonicity and thermal diffuse scattering, the data were collected at 78 K.

Experimental

Large crystals of $Cr(CO)_6$ were easily obtained by sublimation under vacuum. The selected crystal was sealed in a thin-walled quartz tube. The distances of an arbitrary origin inside the crystal to the 18 observed faces were determined, by a least-squares procedure, from the measured lengths of 37 edges. The agreement index $[\sum(l_{obs}-l_{cal})^2/\sum l_{obs}^2]^{1/2}$ (where l_{obs} and l_{cal} are the observed and calculated lengths of the edges) was 0·07.

Data relevant to the crystal and to the experimental conditions are summarized in Table 1.

The numerical values used for the cell dimensions (and which are reported in Table 1) were determined from X-ray diffraction data, rather than from the less precise neutron data, which gave the following values: $a = 11{\cdot}490$ (15), $b = 10{\cdot}905$ (13), $c = 6{\cdot}197$ (14) Å.

Table 1. *Crystal data and experimental conditions*

$Cr(CO)_6$ crystal data
- $M = 220{\cdot}056$
- $\varrho = 1{\cdot}876$ g cm^{-3} at 78 K
- Space group: *Pnma*. $Z = 4$
- Cell dimensions at 78 K (Mo $K\alpha_1$ radiation, $\lambda = 0{\cdot}70930$ Å): $a = 11{\cdot}505$ (4), $b = 10{\cdot}916$ (3), $c = 6{\cdot}203$ (2) Å; $V = 779{\cdot}0$ Å^3
- Cell dimensions at room temperature (Whitaker & Jeffrey, 1967*a*): $a = 11{\cdot}769$ (12), $b = 11{\cdot}092$ (11), $c = 6{\cdot}332$ (6) Å; $V = 826{\cdot}6$ Å^3. True absorption cross section at $\lambda = 1{\cdot}444$ Å and 78 K: $2{\cdot}43 \times 10^{-24}$ cm^2. Incoherent diffusion cross section: $2{\cdot}84 \times 10^{-24}$ cm^2. Total linear 'absorption' coefficient: $\mu = 0{\cdot}0271$ cm^{-1} (Bacon, 1962). Volume of the crystal: 9·3 mm^3. Crystal thickness between 1·8 and 2·9 mm.

Neutron beam
- Monochromator: Cu(111) by transmission
- Wavelength: $\lambda = 1{\cdot}444$ (3) Å
- Contamination by $\lambda/2$: $I_{\lambda/2} = 0{\cdot}0015$ (5) I_λ
- Flux at the sample about 10^6 cm^{-2}s^{-1}
- Detector: BF_3 counter

Mode of data collection
- Maximum $2\theta = 110°$
- $\omega/2\theta$ step scanning. Step in $2\theta = 0{\cdot}06°$
- 2θ interval $= 2[1 + (\tan\theta)/4]°$
- Fixed monitor count: 15000 (which corresponds to about 13s) Largest counting rate: 1300 counts/s (reflexion 400) Two standard reflexions, measured after every 40 reflexions.

The neutron measurements were performed at the Institut Max Von Laue–Paul Langevin of Grenoble, on the diffractometer D10, with cryogenic equipment. The cryogen was liquid helium. A temperature of 78 K was chosen in order to match the temperature of the X-ray experiment, where liquid nitrogen will be used.

The cryostat consists of two spherical shells of aluminum with a vacuum space between. The sample is mounted on the φ axis which turns within the inner shell. This inner space is filled with helium gas which is either static or flowing following the temperature

required. Cooling is provided by a continuous gas flow between a 100 litre helium storage vessel and the crystal by means of a transfer line which has two short flexible sections. The χ movement of the spectrometer produces a rotation of the gas inlet of the cryostat about a circle of radius 12 cm, which is easily followed by the transfer line. The ω movement of the spectrometer is followed in a different fashion. The storage vessel is on a motorized table provided with air cushions. The vessel can be programmed to follow displacements of the ω circle. Since the process is relatively slow, the vessel is moved only to the first point of a scan. The flexibility of the transfer line then allows a step scan of the ω circle without repositioning the vessel. Despite the complication of the mechanics, the advantage of such a system is that the losses in the line are considerably less than those for fully flexible lines. Between 50 K and room temperature helium consumption is less than 4 litres per day.

The gas pressure in the storage vessel is monitored by a pressure sensor which commands a heater if the pressure falls below the set point and which opens a vent if the pressure exceeds the set point by more than about 10 mbar. Typical operating pressure is 130–150 mbar. The temperature of the sample is controlled by a sensor mounted on the heat exchanger block. A small heat input is always provided which varies automatically to compensate for fluctuations in flow rate *etc.* The sample temperature is monitored by a second sensor within the inner sphere. Short term stability of better than 0·1° is common and long term stability of 0·5° is not difficult if a vacuum pump is permanently connected to the cryostat in order to assure constant vacuum conditions.

Data processing

1236 reflexions have been measured (not including the standard reflexions). 106 of them were rejected, because they had been measured in bad conditions (temperature or mechanical instability, *etc.*) or were space-group forbidden. 64 reflexions had been measured twice. After averaging them, there were thus 1066 reflexions for the crystal structure determination, 622 of which were symmetry independent.

Background correction

Diffraction by the aluminum walls of the cryostat causes systematic variations in the background, which makes correction difficult. The variation of the background was studied as a function of the angles 2θ and χ, with the crystal in a non-reflecting position. The background count was obviously a function of 2θ, with rather broad peaks, especially around 39° and 70°, where the background count was about three times its mean value: this is comparable to the counting rate of many weak reflexions of $Cr(CO)_6$. Unfortunately, the background count cannot be described as a function of 2θ alone, nor even of 2θ and χ: the height of the background peaks as well as their position (within about 1°), were dependent on the exact position of the cryostat, and a small change of ω or χ could modify considerably the background intensity. This may be ascribed to the metallic fine texture of the cryostat.

Unless all measurements are repeated after the crystal is removed, it is therefore not possible to know *a priori* the background correction which should be subtracted from each measured value of diffracted intensity. To estimate this correction as precisely as possible, we used a polynomial fit on the observed background counts of each reflexion. This analytical method is described in detail in the Appendix.

$\lambda/2$-contamination

Before reaching the monochromator, the incident neutron beam travels through a long slightly bent guide line where total reflexion occurs for longer wavelengths only, so most of the more energetic neutrons are eliminated. The monochromated beam contains nevertheless a small fraction of neutrons with a wavelength of one half that of the main radiation. From the measurement of space-group forbidden reflexions, this fraction was estimated as 0·15 (5)%.* This is negligible, except for a few weak reflexions *hkl* when the reflexion $2h\ 2k\ 2l$ is very strong. The correction $I_o(2h2k2l)\times 0{\cdot}0015$ was subtracted from the integrated intensity $I_o(hkl)$ of eight reflexions which had an estimated standard deviation σ_c less than this correction, and σ_c^2 was then increased by $[I_o(2h2k2l)\times 0{\cdot}0005]^2$. This correction was applied after the Lorentz correction, and $I_o(2h2k2l)$ was corrected for extinction.

Mean path-length calculation

Absorption is quite negligible (transmission coefficient between 0·994 and 0·997) but the mean path-length $\bar{T}$ was calculated for each reflexion, in view of the extinction corrections. A Gaussian grid of 96 points was found to be sufficient for the numerical integration. For all reflexions, $\bar{T}$ lies between 1·3 and 2·1 mm.

Symmetry-related reflexions

Since neither the mean path-length $\bar{T}$ nor the direction of the relevant vector (for anisotropic extinction corrections) are the same for symmetrical reflexions, these reflexions were *not* averaged. A calculation of symmetry averaging was nevertheless made, in order to obtain a first estimate of the quality of the data set. The agreement between symmetric reflexions is satisfactory: $R=\sum\langle|I_o-\langle I_o\rangle|\rangle/\sum\langle I_o\rangle=0{\cdot}025$, where the summations run over all averaged reflexions, and $\langle\ \rangle$ represents a mean value. This calculation also gives an estimate of the constant p in the expression of the variance: $\sigma^2(I_o)=\sigma_c^2(I_o)+(pI_o)^2$, where σ_c^2 is the

* Throughout this publication, the estimated standard deviation is given in brackets, for the last significant digit.

variance estimated after integration of the peak (see Appendix). From the discrepancy between equivalent reflexions, we obtained $p=0.025$ (3).

Multiple reflexion

Multiple reflexion was checked, using the program *MULREF* (Coppens, 1968), with the following results: for ten strong reflexions, the reciprocal lattice point corresponding to another strong reflexion was within $0.005/\lambda$ of the Ewald's sphere of the incident ray or of the primary diffracted ray, and these reflexions might thus be weakened ('Aufhellung'); on the other hand, four reflexions might be increased by 'Umweganregung' (two reflexions, 231 and $2\bar{3}1$, are present in both groups). Since, for all 12 reflexions, no large or systematic difference was observed between measured and calculated structure factors in the last least-squares refinements, it was concluded that the effect of multiple reflexion is too weak to be of practical importance. A refinement was also carried out omitting these 12 reflexions, with a result which was virtually identical to that of the refinement with the reflexions included.

Crystal structure refinement and extinction corrections

The structure was refined by least-squares calculations, starting from the parameters quoted by Whitaker & Jeffery (1967*a*). The temperature factors have been divided by three, to take into account the difference in temperatures. The full least-squares matrix was used, and the minimized quantity was $\sum w(F^2_{obs}-F^2_{cal})^2$, with: $w^{-1}=\sigma^2=\sigma_c^2+(0.025F^2_{obs})^2$ (see above). The 1066 reflexions were used in the refinement, including those with negative intensity (Hirshfeld & Rabinovich, 1973). The scattering amplitudes were those compiled by Bacon (1972): Cr: 0.352; C: 0.665; O: 0.580, in units of 10^{-12} cm. There are nine atoms in the asymmetric unit, five of which are on the symmetry plane $y=\frac{1}{4}$ (see *Discussion of the space group*).

After determination of the scale factor and two cycles of refinement on all parameters, but no extinction correction, the weighted agreement index $R_w(F^2)=[\sum w(F^2_{obs}-F^2_{cal})^2/wF^4_{obs}]^{1/2}$ was 0.23. Refinement on the extinction parameter g reduced $R_w(F^2)$ to 0.136 (Zachariasen, 1967). It was then noticed that for a few reflexions with high h there was a very large disagreement, the observed intensity being much too low. Unfortunately, the symmetry equivalents of those reflexions had accidentally been omitted in the data collection, so no check was possible. When all reflexions with $h\geq 10$ were rejected from refinement, $R_w(F^2)$ was reduced to 0.056.

It appeared that the reflexions most affected by extinction were undercorrected in Zachariasen's approximation. The extinction correction method recently published by Becker & Coppens (1974*a*,*b*) was then applied. As in Zachariasen's approximation, we used formulae derived for a spherical crystal, but with the true path lengths $\bar{T}$ of the polyhedral crystal. Table 2 gives the results of least-squares refinements with different assumptions on the type of extinction. The value of $R_w(F^2)$ is indicated, and the extinction correction factor y and the corrected intensity F^2_{obs}/k^2y, compared to F^2_{cal}, are given for the two most affected reflexions.

In contrast to Zachariasen's approximation, secondary extinction of type 1 (mosaic-spread dominated) and of type 2 (block-size dominated) is clearly distinguished. As expected, secondary extinc-

Table 2. *Refinements of extinction parameters*

	Extinction parameters ($\times 10^{-4}$)	Scale factor	$\lvert\Delta x/\sigma\rvert$ max	$\lvert\Delta U/\sigma\rvert$ max	Reflexion 400			Reflexion 231			$R_w(F^2)$
					y	F^2_o/y	F^2_c	y	F^2_o/y	F^2_c	
1. Zachariasen	$g=0.80$ (2)	38·31 (12)	0·5	2	0·29	343	401	0·39	240	272	0·0559
2. Primary extinction	$r/\lambda=25.8$ (2)	37·42 (11)	1	6	0·31	329	410	0·39	252	276	0·0596
3. Secondary type 2	$r/\lambda=0.81$ (3)	37·39 (12)	0·8	4	0·31	331	405	0·44	224	275	0·0629
4. Secondary type 1 Gaussian distribution	$g=0.55$ (1)	37·80 (11)	0·5	2	0·20	516	402	0·33	291	273	0·0585
5. Secondary type 1 Lorentzian distribution	$g=0.76$ (1)	38·24 (11)	0·5	2	0·24	413	407	0·32	291	274	0·0553
6. Type 1 anisotropic Lorentzian distribution. Definition of Coppens & Hamilton	$Z_{11}=0.48$ (3) $Z_{22}=0.87$ (6) $Z_{33}=0.61$ (6)	38·28 (11)	0·2	0·5	0·23	420	409	0·32	284	274	0·0548
7. Type 1 anisotropic Lorentzian distribution Definition of Nelmes & Thornley	$Y_{11}=1.99$ (11) $Y_{22}=0.90$ (11) $Y_{33}=1.63$ (15)	38·30 (11)	–	–	0·23	420	409	0·32	285	274	0·0544
8. Type 1 anisotropic Gaussian distribution. Definition of Nelmes & Thornley	$Y_{11}=3.64$ (20) $Y_{22}=1.45$ (20) $Y_{33}=4.45$ (20)	37·87 (11)	0·6	1·3	0·20	495	408	0·29	335	274	0·0594

The non-diagonal elements of the tensors Z and Y are not significantly different from zero. $\lvert\Delta x/\sigma\rvert_{max}$ and $\lvert\Delta U/\sigma\rvert_{max}$ represent the largest shift for position and temperature parameters respectively, divided by the corresponding estimated standard deviation. Refinement 7 is taken as reference.

tion of type 2 and primary extinction have very similar effects: the results would be identical if all $\bar{T}$ were equal, but the refined particle size is very different (Lawrence, 1974): $r_p=(\frac{2}{3}\bar{T}r_s)^{1/2}$, where r_p and r_s represent the mosaic-block radius if extinction is described as primary and as secondary type 2, respectively.

The $Cr(CO)_6$ crystal used is clearly of type 1, with a mosaic-spread distribution nearer to a Lorentzian distribution $[W_L(\varepsilon)=2g/(1+4\pi^2g^2\varepsilon^3)]$ than to a Gaussian distribution $[W_G(\varepsilon)=\sqrt{2g}\exp(-2\pi g^2\varepsilon^2)]$. The same observation was made by Becker & Coppens (1974*b*) for SrF_2. The scale factor is rather strongly dependent on the type of crystal and the mosaic-spread distribution assumed, which shows once more how advantageous would be a direct precise measurement of the scale factor.

In the case of an anisotropic description of the mosaic spread, Nelmes & Thornley (1973) showed, at least for a Gaussian distribution, that the factor g in the expression for $W(\varepsilon)$ should be expressed as $g^2(\mathbf{D})=1/\tilde{\mathbf{D}}\mathbf{Y}\mathbf{D}$, rather than $g^2(\mathbf{D})=\tilde{\mathbf{D}}\mathbf{Z}\mathbf{D}$ (Coppens & Hamilton, 1970). In these expressions, $\mathbf{D}$ is the column matrix of the unit vector normal to the diffraction plane, $\tilde{\mathbf{D}}$ its transpose, and $\mathbf{Y}$ and $\mathbf{Z}$ are symmetrical second order tensors, the elements of which are determined in the least-squares refinement. As is seen in Table 2, the two definitions lead, in our case, to almost identical results, the definition of Nelmes & Thornley seeming slightly better. Compared to an isotropic description, the improvement is small but significant at the 0·5% level, according to the R-ratio significance test of Hamilton (1965), applied to $R_w(F^2)$.

A more careful inspection showed that only eight reflexions, with $h=11$ or 12, had been strongly underestimated in the measurements. These reflexions were given zero weight in a last refinement cycle, carried out assuming a type 1 anisotropic secondary extinction, with the definition of Nelmes & Thornley. In this last cycle, no parameter changed significantly. The final estimated standard deviation of an observation of unit weight was:

$$S=[\sum w(F_{obs}^2-k^2F_{cal}^2)^2/(n_o-n_v)]^{1/2}=1\cdot41,$$

where n_o and n_v are the number of observations (1066) and the number of variables (73), respectively. The relevant agreement indices are:

$$R(F)=\sum|F_{obs}-kF_{cal}|/\sum F_{obs}=0\cdot044;$$
$$R(F^2)=\sum|F_{obs}^2-k^2F_{cal}^2|/\sum F_{obs}^2=0\cdot044;$$
$$R_w(F^2)=[\sum w(F_{obs}^2-k^2F_{cal}^2)^2/\sum F_{obs}^4]^{1/2}=0\cdot052.$$

The relatively high value of $R(F)$, compared to $R(F^2)$ [which is usually about twice as large as $R(F)$] indicates that the precision is much lower for weak reflexions, which is undoubtedly due to imperfect correction of the background fluctuations.

If all reflexions with intensity less than three estimated standard deviations are considered as unobserved, as is done in many crystal structure determinations, these factors become:
$S=1\cdot50$; $R(F)=0\cdot029$; $R(F^2)=0\cdot040$; $R_w(F^2)=0\cdot049$. Compared to the refinement with all reflexions included, there is virtually no change in any of the refined parameters, but the estimated standard deviations are a few per cent higher, owing to the larger value of S.

Sections of the $F_{obs}-F_{cal}$ Fourier synthesis, with all reflexions, were calculated as a check at the end of the least-squares refinement. No residues larger than 0·08 cm^{-1} $Å^{-3}$ were observed (0·12 when the eight 'bad' reflexions are included). For comparison, the largest peaks of the F_{obs} synthesis have a height of about 6 cm^{-1} $Å^{-3}$.

Discussion of the space group

In the preceding sections, the space group *Pnma* was assumed. The reflexion conditions ($h=2n$ on $hk0$ and $k+l=2n$ on $0kl$) cannot discriminate between *Pnma* and $Pn2_1a$. The question of the choice between the two groups has been thoroughly discussed by Whitaker & Jeffery (1967*b*) and our observations and conclusions are similar to theirs. Statistical tests [cumulative distribution $N(Z)$; distribution of the normalized structure factors E] indicate strongly a centrosymmetric structure. Relevant values of the distribution of the E's are given in Table 3.

A least-squares refinement was carried out, in the same conditions as the best refinement in group *Pnma*, but assuming all 13 atoms of $Cr(CO)_6$ to be independent. Since the position of the origin on the y axis is arbitrary, the y coordinate of Cr was fixed at 0·25. Owing to large correlations between the refined y coordinates and between the positional and thermal parameters of 'symmetrical' atoms, the convergence

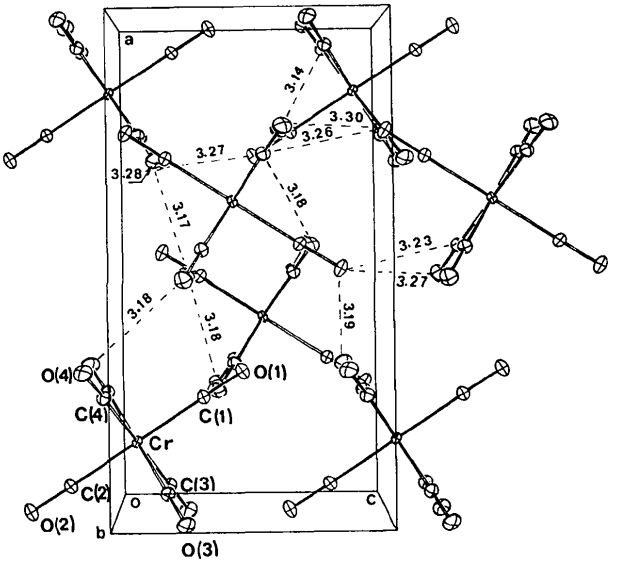

Fig. 1. The crystal unit cell of $Cr(CO)_6$ at 78 K. Thermal ellipsoids are for a 50% probability.

Table 3. *Distribution of the normalized structure factors* (*Stout & Jensen*, 1968)

	$Cr(CO)_6$	Expected *Pnma*	Expected $Pn2_1a$
Average $\|E\|$	0·795	0·798	0·886
Average $\|E^2-1\|$	0·981	0·968	0·736
% reflexions with:			
$\|E\|>1$	31·8	32·0	36·8
$\|E\|>2$	4·8	5·0	1·8
$\|E\|>3$	0·2	0·3	0·01

was slow, and eight cycles were necessary before no parameter (except extinction parameters) varied by more than $0{\cdot}3\sigma$. At the end of the refinement, the agreement values are: $S=1{\cdot}25$; $R(F)=0{\cdot}037$; $R(F^2)=0{\cdot}042$; $R_w(F^2)=0{\cdot}045$. According to Hamilton's test, the improvement is highly significant. But there are large disparities in the amplitudes of thermal motion between chemically equivalent atoms, or, for a given atom, between different directions [the thermal ellipsoid of O(3*a*) is even non-definite]. And equivalent geometrical features vary in a large range: Cr–C length from 1·900 to 1·928 Å; C–O from 1·119 to 1·157 Å; C–Cr–C angle from 178·8 to 179·5°, and from 88·9 to 90·9°; Cr–C–O angle from 177·0 to 179·6°. The agreement between F_{obs} and F_{cal} for the eight reflexions which had to be given zero weight (see above) is no better than in the centrosymmetric refinement. For all these reasons, it may be concluded that the structure is centrosymmetric. This supports the statement of Whitaker & Jeffery (1967*b*), that the *R*-value significance test may lead to erroneous conclusions when the least-squares matrix is ill-defined.

An *a priori* argument against the group $Pn2_1a$ is deduced from the pseudo condition of reflexion $h+2k=4n$ on $hk0$, which is almost exactly verified for all but a few high-angle reflexions. This condition is not only due to the position of Cr, as suggested by Whitaker & Jeffery (1967*a*) – in the neutron data set the contribution of chromium is rather small – but it indicates that the *z* projection of the molecule is nearly symmetric in relation to $x=\frac{1}{8}$. For a regular octahedron, this is only possible if there is a symmetry plane perpendicular to the *y* axis. Even if this symmetry was only approximate, the $Cr(CO)_6$ molecules would probably be randomly distributed, on one side or the other of the plane, throughout the crystal, so there would again be an exact symmetry between the averaged positions. In such a case, the thermal ellipsoids would be more elongated than is observed.

Description of structure and thermal motion

The 13 atoms of $Cr(CO)_6$ were numbered according to Whitaker & Jeffery (1967*a*) and as indicated on the *ORTEP* plot (Fig. 1). The atoms Cr, C(1), O(1), C(2), O(2) are on the symmetry plane.

The relative coordinates and temperature factors, as

Table 4. *Relative coordinates* ($\times 10^5$) *and mean square vibration amplitudes* (*in units of* 10^{-4} Å^2)

The temperature factor is $\exp(-2\pi^2\sum_i\sum_j U_{ij}a_i^*a_j^*)$.

	x	*y*	*z*	U_{11}	U_{22}	U_{33}	U_{12}	U_{13}	U_{23}
Cr	12731 (14)	25000	6153 (25)	81 (9)	59 (7)	59 (7)	0	10 (7)	0
C(1)	21895 (8)	25000	31889 (14)	116 (6)	131 (4)	97 (5)	0	−11 (4)	0
C(2)	3715 (9)	25000	−19712 (14)	118 (6)	131 (4)	106 (5)	0	−21 (4)	0
C(3)	2828 (6)	37337 (5)	18065 (10)	124 (5)	101 (3)	120 (3)	11 (3)	5 (3)	−3 (2)
C(4)	22499 (6)	37524 (5)	−5790 (10)	115 (4)	105 (3)	128 (3)	−12 (2)	3 (3)	17 (2)
O(1)	27354 (10)	25000	47128 (16)	166 (7)	228 (6)	118 (6)	0	−47 (5)	0
O(2)	−1593 (10)	25000	−35257 (16)	183 (7)	224 (6)	112 (6)	0	−52 (5)	0
O(3)	−3157 (8)	44662 (6)	25042 (12)	171 (6)	137 (4)	195 (4)	61 (4)	28 (3)	−26 (3)
O(4)	28167 (7)	45041 (6)	−12931 (11)	159 (5)	156 (4)	216 (5)	−44 (3)	17 (3)	57 (3)

Table 5. *Bond lengths* (Å) *and angles* (°)

Δl is the correction for thermal libration assuming a riding motion of the light atoms around Cr (Busing & Levy, 1964). Estimated standard deviations were computed from the full variance-covariance matrix of least-squares equations and include uncertainty on cell constants (program *ORFFE*).

	l uncorrected	Δl		
Cr—C(1)	1·9132 (18)	0·0034	Cr—C(1)–O(1)	180·00 (10)
Cr—C(2)	1·9105 (18)	0·0037	Cr—C(2)–O(2)	179·46 (11)
Cr—C(3)	1·9125 (13)	0·0029	Cr—C(3)–O(3)	179·37 (8)
Cr—C(4)	1·9185 (13)	0·0031	Cr—C(4)–O(4)	179·10 (7)
C(1)–O(1)	1·1396 (14)	0·0015	C(1)–Cr—C(3)	90·34 (6)
C(2)–O(2)	1·1414 (14)	0·0014	C(1)–Cr—C(4)	89·96 (6)
C(3)–O(3)	1·1406 (10)	0·0018	C(2)–Cr—C(3)	90·06 (6)
C(4)–O(4)	1·1379 (10)	0·0019	C(2)–Cr—C(4)	89·65 (6)
			C(3)–Cr—C(4)	89·79 (3)
			C(3)–Cr—C(3*a*)	89·53 (8)
			C(4)–Cr—C(4*a*)	90·89 (8)
			C(1)–Cr—C(2)	179·44 (10)
			C(3)–Cr—C(4*a*)	179·26 (8)

obtained from the last least-squares refinement with 1066 reflexions, are given in Table 4.

Geometry

The intermolecular distances and angles are given in Table 5. From the differences between chemically equivalent bond angles, it is seen that the $Cr(CO)_6$ octahedron is significantly distorted in the crystal. The differences between the Cr–C bond lengths are small, but Cr–C(4) is longer than the other Cr–C bonds by about 0·006 Å, which could be significant. No significant differences are observed between the C–O bond lengths.

Intermolecular distances

The shortest distances between nuclei in different molecules in the crystal are indicated on Fig. 1. These distances are shorter by about 0·1 Å than at room temperature (Whitaker & Jeffery, 1967*a*).

Thermal motion

A rigid-body analysis, according to Schomaker & Trueblood (1968), showed that the nuclear thermal motion in Table 4 cannot be described as resulting from a rigid-body motion: the root mean square value of $|U_{obs}-U_{cal}|$ was 0·0008 Å, compared to an average estimated $\sigma(U_{obs})$ of about 0·0006 Å, and some $|U_{obs}-U_{cal}|$ residues were as large as $6\sigma(U_{obs})$. This calculation is nevertheless informative. The largest eigenvalue of the translation tensor **T** is 0·0086 (4) Å^2, the corresponding eigenvector being at 9·1° from the *a* axis. The other two eigenvalues are 0·0078 (4) and 0·0073 (4) Å^2. The eigenvalues of the libration tensor **L** are 0·0018 (1) rad^2, at 4·4° from *a* axis, and 0·0013 (1) and 0·0013 (1) rad^2. The motion is thus approximately isotropic, except for an excess squared amplitude of translation of about 0·0010 Å^2 in direction **a**, and an excess squared amplitude of rotation of 0·0005 rad^2 around **a**. The correlation tensor **S** is not significantly different from 0. Only $S_{12}=0{\cdot}00015$ rad Å is larger than the estimated standard deviation (0·00010 rad Å). This means that the chromium nucleus is the effective centre of libration, which of course is not surprising.

Table 6 gives the eigenvalues of the atomic **U** tensors and, for the carbon and oxygen nuclei, the angle of the eigenvector of lowest eigenvalue with the direction of the CO bond. This angle is always very small, even for the carbons [in contrast to the results found by Whitaker & Jeffery (1967*a*)], and the two largest eigenvalues are generally not significantly different. The squared amplitudes of vibration are about four times smaller at 78 K than at room temperature.

The average squared amplitudes of motion of chromium, and the average squared amplitudes of carbon and oxygen in the direction of the CO bond and in a direction perpendicular to CO, are as follows: $U_{Cr}=0{\cdot}0066$ (9); $U_{C\parallel}=0{\cdot}0092$ (2); $U_{O\parallel}=0{\cdot}0086$ (4); $U_{C\perp}=0{\cdot}0128$ (3); $U_{O\perp}=0{\cdot}0215$ (7) Å^2. The standard deviations were estimated from the dispersion of the observed values.

Table 6. *Mean square amplitude of motion along the principal axes of the atomic U tensors*

Units are 10^{-4} Å^2.

	$\overline{u_x^2}$	$\overline{u_y^2}$	$\overline{u_z^2}$	Angle (*Z*,CO)
Cr	85	59	55	–
C(1)	131	122	92	8·2°
C(2)	134	131	90	4·0
C(3)	130	120	96	19·9
C(4)	137	120	90	10·6
O(1)	228	195	89	1·6
O(2)	224	211	84	5·6
O(3)	220	204	79	5·4
O(4)	252	189	90	2·1

Since the root-mean-square amplitude of angular motion around chromium is nearly the same for the carbon and for the oxygen nuclei (3·4° for C and 2·8° for O), it may be assumed that, as a first approximation, each carbonyl group is librating as a whole around chromium. The bond lengths were therefore corrected assuming a riding motion of all C and O atoms around chromium (Table 5; Busing & Levy, 1964). Such corrections are very near to what would be calculated for a rigid-body motion of the whole molecule. Since $U_{C\parallel}$ and $U_{O\parallel}$ are larger than U_{Cr}, there is also a vibrational motion of the carbonyls along the line Cr–C–O. Such a motion cannot be accounted for by a rigid-body description.

Discussion. Refinement of models of geometry and thermal motion

The deformation of the $Cr(CO)_6$ octahedron in the crystal is best seen if the coordinates are expressed in a molecular axial frame. This frame was defined in the following way: if $Cr(CO)_6$ is assumed to be a regular octahedron, the atomic coordinates in the crystal depend only on five parameters: the Cr–C and Cr–O lengths, the coordinates x_0 and z_0 of the centre of the octahedron, and an orientation angle α in the symmetry plane, which was defined as the angle between **a** and the line O(2)–O(1). The 'best' values of the five parameters are determined by least-squares calculations minimizing the differences between 'observed' (those of Table 4) and calculated coordinates, with a weighting scheme based on the standard deviations of Table 4 (correlations between nuclear positions were neglected). The same calculation was done with the positions at room temperature quoted by Whitaker & Jeffery (1967*a*). The angle α was found to be 56·85 (14)° at 78 K and 56·50 (16)° at room temperature. The nuclear coordinates in the molecular frame are then given by:

$$\begin{pmatrix} X \\ Y \\ Z \end{pmatrix} = \begin{pmatrix} a\cos\alpha & 0 & c\sin\alpha \\ a\sin\alpha/\sqrt{2} & b/\sqrt{2} & -c\cos\alpha/\sqrt{2} \\ -a\sin\alpha/\sqrt{2} & b/\sqrt{2} & c\cos\alpha/\sqrt{2} \end{pmatrix} \begin{pmatrix} x-x_0 \\ y-\frac{1}{4} \\ z-z_0 \end{pmatrix}.$$

Table 7 contains the molecular coordinates at 78 K and at room temperature. From this table it is seen that the molecular distortions are very nearly the same in both structure determinations: the coordinates which would be zero for a regular octahedron are always of the same sign, and of similar magnitude.

Table 7. *Molecular coordinates of* $Cr(CO)_6$, *in* $Å \times 10^{-4}$

For definition of molecular axes, see text.

	This work			Whitaker & Jeffery (1967*a*)		
	X	*Y*	*Z*	*X*	*Y*	*Z*
Cr	68	19	−19	27	12	−12
C(1)	19199	89	−89	18930	98	−98
C(2)	−19037	81	−81	−19251	192	−192
C(3)	26	−60	19106	99	−76	19088
C(4)	11	19203	130	21	19102	114
O(1)	30595	130	−130	30441	90	−90
O(2)	−30449	194	−194	−30341	122	−122
O(3)	−116	−156	30510	−201	−128	30450
O(4)	−133	30579	359	−307	30540	205

An other approach would be to determine these five parameters directly from the observed structure factors: in other words, to minimize the quantity $\sum w(F_o^2 - F_c^2)^2$, as in a conventional least-squares refinement, but refining on the five parameters defined above, rather than the 22 independent coordinates of the nuclei. The scale factor, the anisotropic temperature factors and the extinction parameter are refined as usual. (It was found difficult to refine the parameters defining anisotropic extinction, as long as the refinement on the positional and thermal parameters was not quite completed. Therefore, in this and in the subsequent calculations, isotropic extinction was assumed.) The refined values of the five parameters defining the geometry (model 1 of Table 8) were not significantly different from those determined above. The large value of S and $R_w(F^2)$ (see Table 8) shows that this model is not appropriate, and confirms that the octahedron is very significantly distorted.

A more flexible model was then considered (model 2 of Table 8), in which only bond lengths were assumed to be constant. There are then 16 geometrical parameters: x_0 and z_0 of chromium; two parameters for each Cr–C and each Cr–O direction, to define its orientation: the angle with the projection on the symmetry plane (except, of course, for the nuclei which are in the plane) and the angle of this projection with the **a** direction; the lengths Cr–C and Cr–O (since the atoms Cr, C, O are always aligned within 1°, fixing Cr–C and Cr–O also fixes C–O within 0·0001 Å). The values obtained for S and $R_w(F^2)$ in this calculation are very near those of the conventional refinement, although the R-ratio test of Hamilton (1965) indicates that the difference is still significant.

This calculation yields the following values, not corrected for thermal motion, and without consideration of the errors in the cell constants: Cr–C = 1·9148 (4) Å, Cr–O = 3·0538 (5) Å. Corrections for thermal motion may again be made assuming a riding motion of the carbonyls around chromium. With the values of U_{Cr}, $U_{C\perp}$ and $U_{O\perp}$ given by the refinement of model 3 (see below, and Table 8), the calculated corrections are (Busing & Levy, 1964): Δ(Cr–C) = 0·0030 Å and Δ(Cr–O) = 0·0048 Å, and thus the following values may be considered as the best estimates of the average bond lengths in crystalline $Cr(CO)_6$: Cr–C = 1·918 Å; Cr–O = 3·059 Å; C–O = 1·141 Å. These values are in good agreement with those obtained from X-ray diffraction at room temperature by Whitaker & Jeffery (1967*a*), provided the C–O length is corrected for riding motion around chromium, and not around carbon (which seems unrealistic and gives a bond length which is too long): Cr–C = 1·916 Å and C–O = 1·147 Å.

In benzene chromium tricarbonyl, the corrected bond lengths, from neutron diffraction at 78 K (Rees & Coppens, 1973), are Cr–C = 1·845 Å and C–O = 1·158 Å. In free carbon monoxide, the C–O bond length is 1·128 Å (Herzberg, 1966). Thus the C–O bond length in $Cr(CO)_6$ lies between the corresponding lengths in benzene chromium tricarbonyl and in free CO, while the Cr–C bond is appreciably shorter than in the former complex. This is quite in agreement with the well known fact that in benzene chromium tricarbonyl the electronegative carbonyls withdraw

Table 8. *Refinement on simplified geometrical and thermal motion models of* $Cr(CO)_6$

n_v is the number of refined parameters, S the standard deviation of an observation of unit weight, $R(F)$ and $R_w(F_j^2)$ as usual, the other quantities as defined in the text. Isotropic extinction is assumed (type 1, Lorentzian distribution).

	n_v	S	$R(F)$	$R_w(F^2)$	Refined value of some parameters
Conventional refinement	68	1·44	0·045	0·0531	x_{Cr} = 0·12731 (14); z_{Cr} = 0·06148 (25)
Model 1: regular octahedron	51	3·58	0·075	0·133	x_{Cr} = 0·12685 (6); z_{Cr} = 0·06097 (10); α = 56·77 (2)° Cr–C = 1·9151 (9) Å; Cr–O = 3·0524 (11) Å
Model 2: equal Cr–C and equal Cr–O lengths	62	1·46	0·045	0·0542	x_{Cr} = 0·12758 (4); z_{Cr} = 0·06138 (8) Cr–C = 1·9148 (4) Å; Cr–O = 3·0538 (5) Å
Model 3: 5 thermal parameters	29	1·63	0·049	0·061	U_{Cr} = 0·0070 (3); $U_{C\parallel}$ = 0·0098 (3); $U_{O\parallel}$ = 0·0084 (3) $U_{C\perp}$ = 0·0126 (2); $U_{O\perp}$ = 0·0218 (3)
Model 4: 7 thermal parameters	31	1·58	0·048	0·060	U_{Cr} = 0·0064 (3); $U_{C\parallel}$ = 0·0093 (3); $U_{O\parallel}$ = 0·0081 (3) $U_{C\perp}$ = 0·0118 (2); $U_{O\perp}$ = 0·0200 (3) ΔL_{11} = 0·00039 (6) Å × rad²; ΔT_{11} = 0·0019 (3) Å²

electrons, through the chromium atom, from the benzene group: the strength of the Cr–C bond is thus increased, and that of the C–O bonds lowered, owing to partial occupation of the anti-bonding π orbitals of carbon monoxide.

Models describing the thermal motion may be refined in an analogous way. The results are summarized in Table 8. Model 3 considers only the five parameters U_{Cr}, $U_{C\parallel}$, $U_{O\parallel}$, $U_{C\perp}$ and $U_{O\perp}$, defined above, instead of the 44 independent U_{ij}'s in the conventional description with anisotropic motion of the individual nuclei. The R-ratio significance test shows that $R_w(F^2)$ is significantly larger than in the conventional description, and that this simple model provides thus only an approximate description of the thermal motion of the molecules. Model 4 takes two more parameters into account, ΔT_{11} and ΔL_{11}, which are the excess rigid-body mean squared amplitudes, respectively of translation along direction **a** and of libration around an axis parallel to **a**. The improvement over model 3 is significant [$R_w(F^2)$ is lowered by 3%], but the conventional description is still significantly better.

The observed and calculated integrated intensities are shown in Table 9.

APPENDIX

Background correction and peak integration procedure

The problem is to determine analytically the total background B_{peak}, integrated over the same points as the diffraction peak, and to estimate its standard deviation, when there is a systematic variation of the background, due to diffraction by the walls of the cryostat. Since the measurements are made in a step-scanning mode, we try to extrapolate the trends which are observed at each end of the interval of measurements, where the contribution of coherent diffraction by the crystal is negligible.

Let us call B these 'pure background' points, and P the points at the centre of the interval, from which the intensity diffracted by the crystal will be determined. n_B is the number of points B, and n_P the number of points P, such that $N = n_B + n_P$ is the total number of measurements for a given reflexion. Each point is numbered from 1 to N. We try to express the background function as a polynomial of degree m. The calculated background counting rate at point k is thus given by:

Table 9. *Observed and calculated integrated intensities*

The quantities given are: $I_o/100$ (after Lorentz correction), $\sigma(I_o)/100$ (estimated as explained in text) and $F_c^2/100$. The F_c^2's are corrected for extinction and scaled to the I_o's. A standard deviation of zero means that zero weight was given to the reflexion during least-squares refinement.

$$C_{k,\mathrm{cal}}=\sum_{l=0}^{m} A_l k^l$$

The coefficients A_l are obtained by least-squares fit to the observed background rates $C_{k,\mathrm{obs}}$ of the points B. Since the estimated variance for a Poisson distribution is $C_{k,\mathrm{obs}}$, the weight of each point will be $1/C_{k,\mathrm{obs}}$. The least-squares matrix $\mathbf{Q}$ is of order $m+1$, and its general element is:

$$Q_{ij}=\sum_{k}^{B} k^{i+j-2}/C_{k,\mathrm{obs}}$$

where the summation is taken over all points B. The polynomial coefficients are:

$$A_i=\sum_{j=0}^{m}(Q^{-1})_{i+1,j+1}\sum_{k}^{B} k^j.$$

The estimated variance of an observation of unit weight is:

$$S^2=[\sum_{k}^{B}(C_{k,\mathrm{obs}}-C_{k,\mathrm{cal}})^2/C_{k,\mathrm{obs}}]/(n_B-m-1)$$

and $S^2\mathbf{Q}^{-1}$ is the estimated variance-covariance matrix of the A_l's.

Since each $C_{k,\mathrm{obs}}$ may be considered as the value of a normally distributed random variable (the Poisson and normal distributions being practically identical for the observed counting rates), $(n_B-m-1)S^2$ may be tested against the χ^2 distribution with (n_B-m-1) degrees of freedom.

An estimation of the integrated background under the n_P points P is then given by:

$$B_{\mathrm{peak}}=\sum_{k}^{P} C_{k,\mathrm{calc}}=\mathbf{MA}\,,$$

where the summation is taken over all points P, $\mathbf{M}$ is the matrix $[\sum_{k}^{P} k^0 \sum k^1 \ldots \sum k^m]$, and $\mathbf{A}$ the column matrix of the polynomial coefficients. The estimated variance is

$$\sigma^2(B_{\mathrm{peak}})=\mathbf{M}S^2\mathbf{Q}^{-1}\tilde{\mathbf{M}}\,.$$

The total integrated intensity and its estimated variance is as usual:

$$I_{\mathrm{tot}}=\sigma^2(I_{\mathrm{tot}})=\sum_{k}^{P} C_{k,\mathrm{obs}}$$

A Fortran program was written, which does the following for each reflexion.

(1) *Separation between points B and points P*

The reflexion peak is first carefully centred, considering the point of maximum counting rate and the points of half-height of the peak. An equal number of points P is taken on each side of this centre, knowing the total width of the peak, which was previously determined as a function of the 2θ angle and, for the most intense reflexions, of the intensity.

It was found later, during the crystal structure determination, that this procedure tended to overestimate the weak reflexions when diffraction by the cryostat was present in the background: the peak was then shifted away from its expected position (the mid-point of the interval), and its half-width was not in agreement with a previously determined curve. This was checked in a second run, and when such an anomalous behaviour was detected, the peak was assumed to be centred at the mid-point, and its total width increased by 0·2° on each side.

(2) *Polynomial fit*

The hypothesis of a constant background ($m=0$) is first tried. If $(n_B-1)S^2$ is significantly larger than what would be expected for a χ^2 distribution at a 5% level of significance, and if n_B is at least equal to 10 (which was verified for almost all reflexions), a parabolic fit is tried ($m=2$), and $(n_B-3)S^2$ again tested against χ^2. If the agreement is not significantly better, the results of the constant background hypothesis are taken. Note that, even if a constant background is assumed, the variance of the total background depends, through S^2, on the observed fluctuations. This seems more realistic than the simple consideration of the counting error of each separate point, as is usually done.

(3) *Integrated intensity*

The corrected integrated intensity is:

$$I=I_{\mathrm{tot}}-B_{\mathrm{peak}}$$

and its estimated variance, due to counting and background errors:

$$\sigma_c^2(I)=I_{\mathrm{tot}}+K\sigma^2(B_{\mathrm{peak}})$$

The coefficient K was introduced to take into account the imprecision resulting from imperfect corrections, and was taken larger in regions where important fluctuations were observed. We fixed, somewhat arbitrarily: $K=2$ throughout the reciprocal space; $K=4$ in the intervals 31 to 47° and 57 to 77° in 2θ; $K=8$ in the intervals 38 to 40° and 69 to 72°.

Results

30% of the reflexions were integrated assuming a parabolic variation. Two of them were found to be badly integrated, because there were no background points on one side of the peak. These were integrated again with the assumption of a constant background. For 16% of the reflexions treated with parabolic integration, $(n_B-3)S^2$ was larger than the maximum value of χ^2 at the 5% probability level. This indicates that the parabolic background description, although satisfactory for most reflexions, is not quite adequate for a few of them. But the number of background points would probably be insufficient for the use of a polynomial of higher degree.

References

BACON, G. E. (1962). *Neutron Diffraction*, 2nd ed. Oxford: Clarendon Press.
BACON, G. E. (1972). *Acta Cryst.* A**28**, 357–358.
BECKER, P. J. & COPPENS, P. (1974*a*). *Acta Cryst.* A**30**, 129–147.
BECKER, P. J. & COPPENS, P. (1974*b*). *Acta Cryst.* A**30**, 148–153.
BUSING, W. R. & LEVY, H. A. (1964). *Acta Cryst.* **17**, 142–146.
COPPENS, P. (1968). *Acta Cryst.* A**24**, 253–257.
COPPENS, P. & HAMILTON, W. C. (1970). *Acta Cryst.* A**26**, 71–83.
HAMILTON, W. C. (1965). *Acta Cryst.* **18**, 502–510.
HERZBERG, G. (1966). *Spectra of Diatomic Molecules*. Princeton: Van Nostrand.
HIRSHFELD, F. L. & RABINOVICH, D. (1973). *Acta Cryst.* A**29**, 510–513.
LAWRENCE, J. L. (1974). *Acta Cryst.* A**30**, 454–455.
NELMES, R. J. & THORNLEY, F. R. (1973). *First European Congress of Crystallography*, Abstract Group B1. Bordeaux.
REES, B. & COPPENS, P. (1973). *Acta Cryst.* B**29**, 2516–2528.
SCHOMAKER, V. & TRUEBLOOD, K. N. (1968). *Acta Cryst.* B**24**, 63–76.
STOUT, G. H. & JENSEN, L. H. (1968). *X-ray Structure Determination*, p. 321. New York: Macmillan.
WHITAKER, A. & JEFFERY, J. W. (1967*a*). *Acta Cryst.* **23**, 977–984.
WHITAKER, A. & JEFFERY, J. W. (1967*b*). *Acta Cryst.* **23**, 984–989.
ZACHARIASEN, W. H. (1967). *Acta Cryst.* **23**, 558–564.

Acta Cryst. (1975). B**31**, 2658

Die Struktur des 4,4′-Dimethoxy-α,β-diäthylstilbens

VON GERHARD RUBAN UND PETER LUGER

Freie Universität Berlin, Institut für Kristallographie, 1 *Berlin* 33, *Takustrasse* 6, *Deutschland* (*BRD*)

(*Eingegangen am* 18. *September* 1974; *angenommen am* 18. *April* 1975)

4,4′-Dimethoxy-α,β-diethylstilbene is monoclinic, $a=10{\cdot}753\pm0{\cdot}005$, $b=24{\cdot}096\pm0{\cdot}004$, $c=7{\cdot}853\pm0{\cdot}006$ Å, $\beta=123{\cdot}09\pm0{\cdot}02°$, space group $P2_1/n$ (C_{2h}^5) with four molecules per unit cell. The intensities of 3210 independent reflexions were collected on an automatic diffractometer. The structure was solved by statistical methods. Least-squares refinement of the positional and thermal parameters led to a final R value of 5·1 %. This compound is the first stilbene derivative with oestrogenic activity in a non-centrosymmetric molecular configuration. This is caused by the terminal carbon atoms of the ethyl groups being on the same side of the plane formed by the atoms which are linked to the central double bond.

Durch die Arbeiten von Dodds, Golberg, Lawson & Robinson (1939) sind verschiedene, verhältnismässig einfach gebaute synthetische Verbindungen bekannt geworden, die die gleichen physiologischen Wirkungen wie die Follikelhormone zeigen. Sie leiten sich vornehmlich vom Stilben und Dibenzyl ab.

Zahlreiche Untersuchungen wurden mit den verschiedensten Methoden angestellt, um den Zusammenhang zwischen physiologischer Wirksamkeit und stereochemischem Aufbau dieser Verbindungen aufzuklären. Von den Kristallstrukturaufklärungen sind insbesondere die am Diäthylstilböstrol (Weeks, Cooper & Norton, 1970) und am Dienöstrol (Forniés-Marquina, Busetta & Hospital, 1972) zu erwähnen. In beiden Fällen handelt es sich um Moleküle, bei denen ein Symmetriezentrum kristallographisch erzwungen wird. Dies betrifft insbesondere die Substituenten an der mittleren C–C-Brücke, die dadurch nicht mehr verschiedene, voneinander unabhängige Anordnungen besitzen können.

Grundlage dieser Arbeit ist das 4,4′-Dimethoxy-α,β-diäthylstilben, der Dimethyläther des Diäthylstilböstrols, von dem bereits Elementarzelle* und Raumgruppe bekannt waren (Bötticher, 1959). Danach musste das Molekül entweder ohne Eigensymmetrie

* Im Drück hinzugefügt: Die Gitterkonstanten wurden bereits publiziert von Bötticher, Plieth & Repmann (1965).

Tabelle 1. *Kristalldaten*

4,4′-Dimethoxy-α,β-diäthylstilben
Summenformel: $C_{20}H_{24}O_2$
Masse der Formeleinheit: 296,4

Gitterkonstanten:
$a=10{,}753\pm0{,}005$ Å
$b=24{,}096\pm0{,}004$
$c=7{,}853\pm0{,}006$
$\beta=123{,}09°\pm0{,}02°$
$V=1704{,}7$ Å^3

$\varrho_{exp}=1{,}15\pm0{,}03$ g cm^{-3} (Schwebemethode)
$\varrho_x=1{,}16$
$Z=4$
Raumgruppe $P2_1/n$ (C_{2h}^5)
$\mu=6{,}8$ cm^{-1} für Cu $K\alpha$-Strahlung